OXFORD GENETICS

GENETICS, 2022, 220(1), iyab198
https://doi.org/10.1093/genetics/iyab198
Advance Access Publication Date: 6 November 2021
Neurogenetics

A conserved behavioral role for a nematode interneuron neuropeptide receptor

Cynthia M. Chai ,† Wen Chen,† Wan-Rong Wong,† Heenam Park, Sarah M. Cohen, Xuan Wan , and Paul W. Sternberg *

Division of Biology and Biological Engineering, California Institute of Technology, Pasadena, CA 91125, USA

*Corresponding author: Email: pws@caltech.edu
†These authors contributed equally to this work.

Downloaded from https://academic.oup.com/genetics/article/220/1/iyab198/6422542 by guest on 18 April 2024

Abstract

Neuropeptides are evolutionarily conserved modulators of many aspects of animal behavior and physiology, and expand the repertoire of processes that can be controlled by a limited number of neurons. Deciphering the neuropeptidergic codes that govern distinct processes requires systematic functional analyses of neuropeptides and their cognate receptors. Even in well-studied model organisms like *Caenorhabditis elegans*, however, such efforts have been precluded by a lack of mutant reagents. Here, we generated and screened 21 *C. elegans* neuropeptide G-protein coupled receptor mutants with no pre-existing reagents for the touch-evoked escape response, and implicated six receptors expressed in diverse neuron classes representing multiple circuit levels in this behavior. We further characterized the mutant with the most severe phenotype, *frpr-14*, which was defective in multiple behavioral paradigms. We leveraged this range of phenotypes to reveal that FRPR-14 modulation of different precommand interneuron classes, AVH and AIB, can drive distinct behavioral subsets, demonstrating cellular context-dependent roles for FRPR-14 signaling. We then show that *Caenorhabditis briggsae* CBR-FRPR-14 modulates an AVH-like interneuron pair to regulate the same behaviors as *C. elegans* but to a smaller extent. Our results also suggest that differences in touch-evoked escape circuit architecture between closely related species results from changes in neuropeptide receptor expression pattern, as opposed to ligand–receptor pairing. This study provides insights into the principles utilized by a compact, multiplexed nervous system to generate intraspecific behavioral complexity and interspecific variation.

Keywords: neuropeptide; interneurons; locomotion; G-protein coupled receptor; *Caenorhabditis briggsae*; escape behavior; *Brugia malayi*; *Onchocerca volvulus*; neurogenetics

Introduction

Predation is a major evolutionary selective force that sculpts the form and function of prey circuits. To enhance prey survival chances, escape sensorimotor circuits are designed to execute fast, robust behavioral responses that promote successful capture evasion (Card 2012; Herberholz and Marquart 2012). While foraging, the microscopic *Caenorhabditis elegans* may encounter predators like nematophagous mites (Karagoz *et al.* 2007), fungi (Xie *et al.* 2010; Maguire *et al.* 2011; Yang *et al.* 2020), and even other nematode species like *Pristionchus pacificus* (Bento *et al.* 2010; Wilecki *et al.* 2015). Tactile stimulation during these dangerous encounters triggers bidirectional undulatory movements away from the threat that are mediated by *C. elegans*' head and body touch-evoked escape circuits (Chalfie and Sulston 1981; Chalfie *et al.* 1985; Kaplan and Horvitz 1993; Piggott *et al.* 2011; Pirri and Alkema 2012). The touch-evoked escape response can be modified by different behavioral states (Chao *et al.* 2004; Schwarz *et al.* 2011; Cho and Sternberg 2014) and in some cases, neuropeptide signaling has been implicated in driving this state-dependent modulation (Choi *et al.* 2013; Chen and Chalfie 2014; Nath *et al.* 2016).

However, a comprehensive understanding of how extrasynaptic neurohormonal networks modulate *C. elegans* behavior and physiology has been hindered by a lack of mutant reagents. To address this, we used a CRISPR homology-directed repair strategy to generate putative null mutants for the 12 *frpr* (FMRFamide-like peptide receptor) and 9 *npr* (neuropeptide receptor) neuropeptide G-protein coupled receptors with no pre-existing mutant reagents (Wang *et al.* 2018). The *npr* and *frpr* families are two of the largest annotated neuropeptide GPCR-encoding gene families in *C. elegans* and many members have reported behavioral phenotypes (reviewed in Frooninckx *et al.* 2012). Of the 21 receptor genes selected for knockout in this study, only *npr-6* has a previously associated behavioral phenotype (egg-laying defective) identified through RNAi knockdown (Keating *et al.* 2003).

Materials and methods

Animal maintenance and strains

Animals were cultivated at 20°C on standard nematode growth media (NGM) plates seeded with *Escherichia coli* OP50 cultured in Luria-Bertani broth. The following strains were used in this study:

Received: August 24, 2021. **Accepted:** October 28, 2021
© The Author(s) 2021. Published by Oxford University Press on behalf of Genetics Society of America. All rights reserved.
For permissions, please email: journals.permissions@oup.com

N2 (Bristol)
AF16 (India)
PS8429: *frpr-14(sy1301)*
PS8430: *frpr-17(sy1302)*
PS8487: *frpr-8(sy1363)*
PS8400: *frpr-7(sy1296)*
PS8484: *npr-31(sy1360)*
PS8450: *npr-27(sy1315)*
PS8490: *frpr-16(sy1366)*
PS8432: *frpr-19(sy1304)*
PS8488: *frpr-2(sy1364)*
PS8398: *frpr-9(sy1294)*
PS8315: *npr-29(sy1270)*
PS8444: *npr-21(sy1309)*
PS8442: *npr-26(sy1307)*
PS8330: *frpr-5(sy1274)*
PS8426: *frpr-13(sy1298)*
PS8317: *npr-33(sy1272)*
PS8396: *frpr-1(sy1292)*
PS8177: *npr-23(sy1203)*
PS8334: *frpr-11(sy1278)*
PS8938: *frpr-12(sy1581)*
PS8902: *npr-6(sy1571)*
PS7379: *flp-3(ok3265)*
PS9050: *flp-4(sy1606)*
VC2324: *flp-6(ok3056)*
PS9098: *flp-3(ok3265); frpr-14(sy1301)*
PS9056: *flp-4(sy1612); frpr-14(sy1301)*
PS9099: *flp-6(ok3056); frpr-14(sy1301)*
PS9138: *syEx1857* [*Pfrpr-1::GFP*; *Pnmr-1::mCherry-H2B*, *Pofm-1::RFP*]
PS9139: *syEx1858* [*Pfrpr-5::GFP*; *Pnmr-1::mCherry-H2B*, *Pofm-1::RFP*]
PS9140: *syEx1859* [*Pfrpr-12::GFP*; *Pnmr-1::mCherry-H2B*, *Pofm-1::RFP*]
PS9141: *syEx1860* [*Pnpr-29::GFP*; *Pnmr-1::mCherry-H2B*, *Pofm-1::RFP*]
PS9142: *syEx1861* [*Pnpr-31::GFP*; *Pnmr-1::mCherry-H2B*, *Pofm-1::RFP*]
PS9146: *syEx1862* [*Pflp-3::GFP*; *Pmec-4::mCherry-H2B*, *Pofm-1::RFP*]
PS8948: *syEx1789* [*Pfrpr-14::frpr-14* gDNA::SL2::*GFP*, *Phlh-34::mCherry-H2B*, *Pofm-1::RFP*]; *sy1301*
PS8927: *syEx1785* [*Pfrpr-14::frpr-14* gDNA::SL2::*GFP*, *Pnpr-9::mCherry-H2B*, *Pofm-1::RFP*]; *sy1301*
PS8957: *syEx1795* [*Phlh-34::frpr-14* cDNA::SL2::*GFP*, *Pofm-1::RFP*]; *sy1301*
PS8946: *syEx1787* [*Pnpr-9::frpr-14* cDNA::SL2::*GFP*, *Pofm-1::RFP*]; *sy1301*
PS8984: *syEx1803* [*Phlh-34::Cbr-frpr-14* cDNA::SL2::*GFP*, *Pofm-1::RFP*]; *sy1301*
PS9003: *syEx1808* [*Phlh-34::Bma-frpr-14* cDNA::SL2::*GFP*, *Pofm-1::RFP*]; *sy1301*
PS9103: *syEx1841* [*Phlh-34::Ovo-frpr-14* cDNA::SL2::*GFP*, *Pofm-1::RFP*]; *sy1301*
PS9001: *Cbr-frpr-14(sy1601)*
PS9000: *Cbr-frpr-14(sy1602)*
PS8977: *syEx1796* [*PCbr-frpr-14::Cbr-frpr-14* gDNA::SL2::*GFP*]
CB1490: *him-5(e1490)*
CB169: *unc-31(e169)*

Molecular biology and transgenesis

frpr-14 cDNA was PCR amplified from N2 cDNA library. Gene promoters and *frpr-14* genomic DNA were PCR amplified from N2 genomic DNA library. *Cbr-frpr-14* genomic DNA was PCR amplified from AF16 genomic DNA library. Promoters for generating transcriptional reporters are *hlh-34* (2.6 kb), *npr-9* (2.0 kb), *frpr-1* (2.5 kb), *frpr-5* (2.5 kb), *frpr-12* (1.1 kb), *npr-29* (2.5 kb), *npr-31* (3.0 kb), *nmr-1* (4.7 kb), *mec-4* (250 bp), and *flp-3* (1.5 kb). The entire *C. elegans frpr-14* genomic locus including 600 bp of regulatory region upstream of the start codon was used to generate the *frpr-14* translational GFP fusion. The entire *C. briggsae Cbr-frpr-14* genomic locus including 570 bp of regulatory region upstream of the start codon was used to generate the *Cbr-frpr-14* translational GFP fusion. *Cbr-frpr-14* (CBG19545), *Bma-frpr-14* (Bm4879a), and *Ovo-frpr-14* (OVOC11602) cDNA constructs were synthesized by Integrated Data Technologies gBlocks. Constructs were inserted into either pSM *GFP* or pSM *mCherry-H2B* vector backbone using HiFi Assembly or restriction enzyme cloning.

Transgenic strains were generated by microinjection of plasmids with coinjection markers into adult worms. cDNA plasmids were injected at 50 ng/μl. GFP and mCherry reporter constructs were injected at 25–50 ng/μl. Coinjection marker *Pofm-1::RFP* was injected at 40 ng/μl. One kilobase of DNA ladder was used as a filler to bring final DNA concentration to 200 ng/μl.

CRISPR mutagenesis

CRISPR mutagenesis in *C. elegans* was performed as previously described (Wang *et al.* 2018). CRISPR mutagenesis in *C. briggsae* was performed as previously described (Cohen and Sternberg 2019). Briefly, a 43-bp universal STOP-IN cassette was inserted near the target gene's 5′ end to disrupt translation. Independent F2 homozygous animals were isolated using PCR detection and confirmed with Sanger sequencing.

Posterior body gentle touch-evoked escape response assay

Ten L4 stage worms were picked to seeded NGM plates and allowed to lay eggs for 2 h before being removed. Plates were incubated at 20°C until worms reached the young adult stage. On each plate, ten worms were scored individually for the posterior body touch-evoked escape response. Using an eyelash pick, each worm was gently touched on the anterior body region immediately posterior to the pharynx to trigger a reversal. Immediately after the reversal motor program terminated, worms were touched on the posterior body region. Whether or not the worm responded to this posterior touch by moving forward was recorded. This procedure was repeated 10 times per animal with a time interval of 5 s in between trials. The response rate for each worm is the percentage of positive responses (forward movements) out of 10 trials. The average response per batch is the average of response rates for the ten worms assayed per plate. At least three batches were assayed per strain. All assays were conducted at 22°C.

Two independent F1 transgenic lines were assayed for each touch-evoked escape rescue experiment. In all touch-evoked escape rescue experiments, both independent F1 transgenic lines rescued the *frpr-14(−)* mutant's defect to similar extents (not statistically significant from each other). We then selected the F1 transgenic line with the highest array transmission rate for further investigation using the motility assay described below.

Motility assay

L4 stage animals were picked around 16 h before experiments and grown at 20°C overnight. On the day of experiments, experimental plates were seeded with a saturation-phase culture of *E. coli* OP50. Plates were left to dry at room temperature for 1–2 h. Four to six young adults were then picked onto each experimental plate and left to acclimatize for at least 30 min at room temperature. Each plate was then video recorded for 4 min at 7.5 frames/s using the MBF Bioscience WormLab setup. The camera

Downloaded from https://academic.oup.com/genetics/article/220/1/iyab198/6422542 by guest on 18 April 2024

field of view was centered on each food patch. All recordings were conducted within 30–60 min after worms were transferred to experimental plates. Videos were analyzed using WormLab software with the following mobility idle time analysis settings—speed threshold: 1.5 μm/s, averaging window: five frames, minimum duration: five frames. As animals sometimes move out of the field of view during video recording, each animal's total mobility idle time was normalized by total track duration to obtain the percentage of mobility idle time. All assays were conducted at 22°C.

Male mating assays

L4 stage males and L4 stage *unc-31* hermaphrodites were picked to separate seeded NGM plates and grown at 20°C overnight. NGM plates were spotted at the center with 10 μl of concentrated *E. coli* OP50 and dried overnight at room temperature. On the day of experiments, 15 adult *unc-31* hermaphrodites were picked onto the bacteria lawn of each mating plate. Three adult males were then placed onto the bacteria lawn with the hermaphrodites and behavior was video recorded for 4 min. The mating behaviors of each male were manually scored throughout this duration using the following criteria:

- *Touch response assay*
  a) Touch not leading to mating response: ventral side of male tail makes touch contact with hermaphrodite but male does not initiate backing.
  b) Touch leading to mating response: ventral side of male tail makes touch contact with hermaphrodite and male initiates backing.
- *Vulva location assay*
  a) Successful vulva location: male stops for >1 s at vulva.
  b) Vulva pass: male does not stop at vulva.
  c) Hesitation: male pauses at vulva for <1 s but then moves away.

All assays were conducted at 22°C.

Microscopy

Animals were immobilized with 100 mM sodium azide on 2% agarose pads. Slides were imaged under a ZEISS Axio Imager.Z2 microscope attached to a Axiocam 506 mono microscope camera. Images were processed using ZenPro software.

Statistical analysis

For touch-evoked escape assays, unpaired Welch's *T*-test or ANOVA followed by Tukey HSD *post hoc* analysis were used to determine statistically significant differences between groups. For motility assays, Kruskal–Wallis test followed by Dunn's *post hoc* with Holm–Bonferroni correction was used to determine statistically significant differences between groups. For male-mating assays, Wilcoxon rank sum test was used to determine statistically significant differences between groups. All *P*-values reported in the figure legends are corrected *P*-values. Statistical analyses were performed in R. Plots were generated in Python.

Results and discussion

To generate neuropeptide GPCR mutants, a triple stop cassette was inserted in-frame near the 5′ end of each predicted receptor-encoding gene sequence. All 21 neuropeptide receptor mutants generated here did not exhibit observable abnormalities in developmental growth rate. We behaviorally screened this set of mutants using the posterior body gentle touch-evoked escape response assay. In this assay, an eyelash pick was used to gently stroke the animal's anterior body region immediately behind the pharynx to elicit a reversal (Figure 1A). At the end of the reversal sequence, another gentle touch stimulus is delivered to the tail region within the PLM touch receptor neurons' sensory field, and whether or not a forward movement occurs is recorded (Figure 1A). This procedure was repeated ten consecutive times for each animal and the percentage of forward movement responses per animal is calculated. The response rates of 10 animals were then averaged to obtain each batch average response. Our screen revealed touch-evoked escape defective phenotypes for six receptor mutants—*frpr-1*, *frpr-5*, *frpr-12*, *frpr-14*, *npr-29*, and *npr-31* (Figure 1B). We next generated transcriptional GFP reporters for these receptors and analyzed the extent of expression pattern overlap with the body gentle touch-evoked escape circuit consisting of the ALM, AVM, PVM, PLM touch sensors, the AVA, AVB, AVD, PVC command interneurons, and motor neurons (Chalfie and Sulston 1981; Chalfie *et al.* 1985; Chatzigeorgiou *et al.* 2010). While *frpr-5* and *frpr-12* expression is largely restricted to canonical circuit elements such as premotor command interneurons and body touch receptor neurons, the other four receptors are expressed in diverse neuron classes including chemosensory neurons and noncommand interneurons (Figure 1C). Taken together, these observations indicate that the neural circuitry underlying the body touch-evoked escape response is more distributed than previously thought and is modulated at multiple circuit levels by neuropeptide signaling.

As *frpr-14* mutants had the most severe touch-evoked escape response defect compared with control animals, we chose to further characterize the neurobehavioral role of this receptor. During food patch exploration in search of mating partners, *C. elegans* males use specialized tail ray structures to detect hermaphrodite-specific structural and chemical features leading to initiation and execution of the male mating behavior sequence (Liu and Sternberg 1995; Barr and Sternberg 1999). Upon touch contact with and successful recognition of the hermaphrodite, the male uses its tail to travel along the hermaphrodite's body length until it locates the vulva and copulates (Liu and Sternberg 1995). We found that *frpr-14* mutant males are deficient at initiating the mating sequence upon touch contact with the hermaphrodite (Supplementary Figure S1, A and B) and vulva location (Supplementary Figure S1, C and D) demonstrating a sexually dimorphic role for FRPR-14 in male mating.

During routine animal maintenance, we observed that *frpr-14* mutants exhibit prolonged bouts of locomotion quiescence compared with wild-type N2 animals. Using an automated freely moving behavior recording and analysis setup, we quantified this spontaneous motility defect as the percentage of recording time the animal did not exceed a specified bidirectional movement distance threshold (henceforth called "mobility idle time"). Under these conditions, *frpr-14* mutants show a significantly greater mobility idle time relative to controls (Figure 1, D–F). We also note that while *frpr-14* mutants are able to spontaneously execute bidirectional movement, they are slow and uncoordinated when so doing.

Based on colocalization analysis using AVH- and AIB-specific markers, respectively, we determined that a *frpr-14* translational GFP reporter was expressed in the AVH and AIB interneuron classes (Figure 2A; Supplementary Figure S2, A and B) (Bendena *et al.* 2008; Cook *et al.* 2021). Neither neuron class has a reported role in the body touch-evoked escape response. To determine receptor site of action, we expressed functional copies of *frpr-14* in a

Downloaded from https://academic.oup.com/genetics/article/220/1/iyab198/6422542 by guest on 18 April 2024

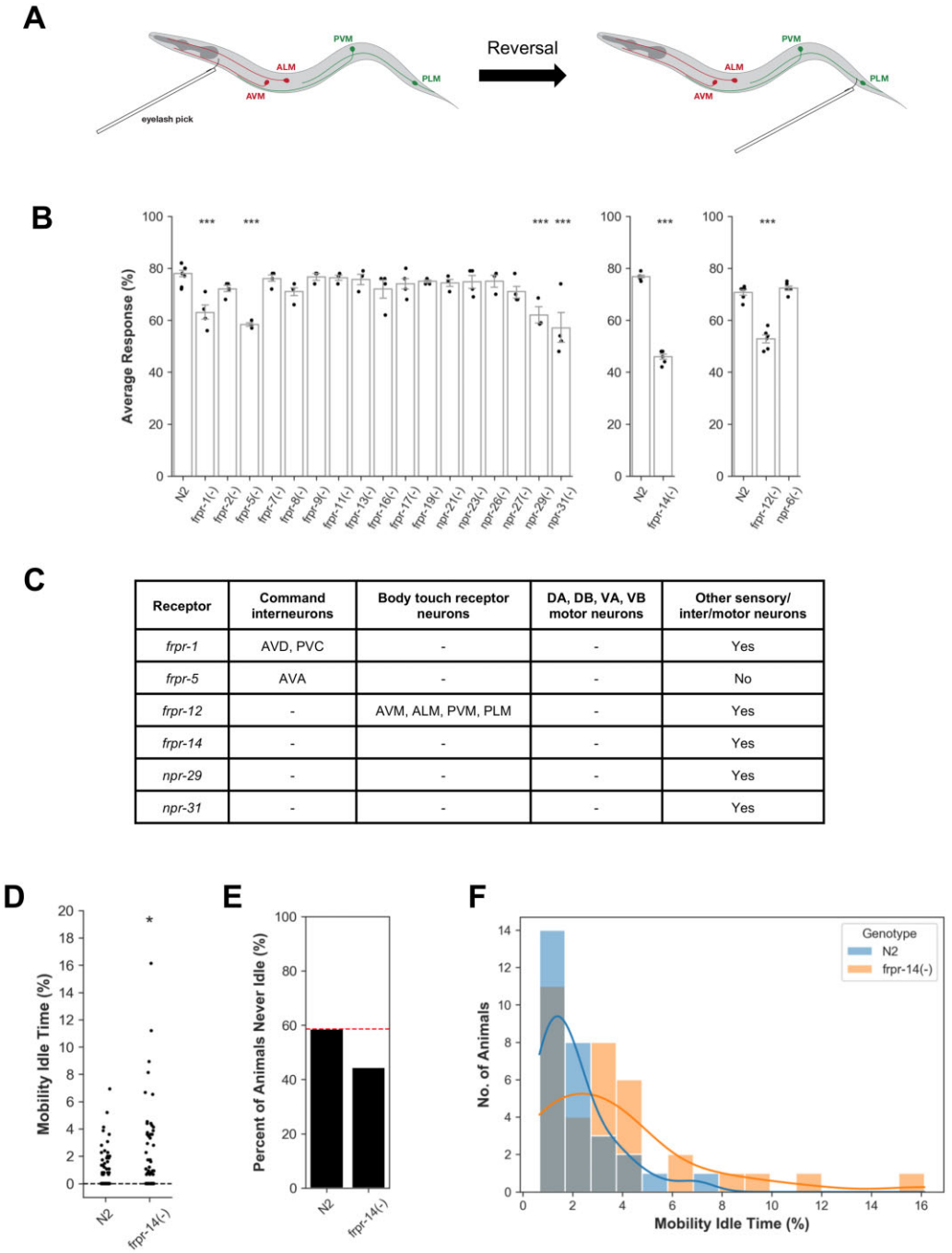

Receptor	Command interneurons	Body touch receptor neurons	DA, DB, VA, VB motor neurons	Other sensory/ inter/motor neurons
frpr-1	AVD, PVC	-	-	Yes
frpr-5	AVA	-	-	No
frpr-12	-	AVM, ALM, PVM, PLM	-	Yes
frpr-14	-	-	-	Yes
npr-29	-	-	-	Yes
npr-31	-	-	-	Yes

Figure 1 Multilevel modulation of the body touch-evoked escape circuit by neuropeptide signaling. (A) Schematic of posterior body gentle touch-evoked escape assay. Drawing not to scale. (B) Touch-evoked escape response assay screen of neuropeptide GPCR putative null mutants. Error bars represent standard error of the mean. $N = 3$–8 batches. One-way ANOVA followed by Dunnett's *post hoc* compared with N2. Unpaired Welch's *t*-test for N2—*frpr-14*(−) pairwise comparison. ***$P < 0.001$. *frpr-1*(−) ($P = 1.7e{-}04$), *frpr-5*(−) ($P = 5.7e{-}06$), *frpr-12*(−) ($P = 4.5e{-}08$), *frpr-14*(−) ($P = 1.0e{-}08$), *npr-29*(−) ($P = 3.0e{-}04$), *npr-31*(−) ($P = 5.9e{-}08$). (C) Summary of touch-evoked escape defective receptor expression patterns. Data derived from *frpr-1*, *frpr-5*, *frpr-12*, *npr-29*, *npr-31* transcriptional GFP reporter strains coexpressing a *Pnmr-1::mCherry-H2B* command interneuron marker (Zheng *et al.* 1999), and *frpr-14* translational GFP reporter strains coexpressing either a *Phlh-34::mCherry-H2B* AVH-specific marker (Cook *et al.* 2021) or a *Pnpr-9::mCherry-H2B* AIB-specific marker (Bendena *et al.* 2008) (see Supplementary Fig S2, A and B for images). Presence or absence of AVB interneurons determined by soma position relative to AVD (as marked by *Pnmr-1::mCherry-H2B*) and process morphology. (D) Percentage of mobility idle time throughout recording duration. $N = 63$–70 animals. Wilcoxon rank sum test. *$P < 0.05$. $P = 2.622e{-}02$. (E) Percent of animals in (D) that were never idle (*i.e.*, Mobility Idle Time = 0). (F) Distribution of nonzero mobility idle times in (D). Colored lines represent kernel density estimation. $N = 29$–35 animals.

neuron class-specific manner in *frpr-14* mutants and assayed transgenic animals using both the touch-evoked escape response and motility assays. We found that either AVH- or AIB-specific expression was sufficient to fully reinstate the mutant's touch-evoked escape response (Figure 2B), while only AVH-specific expression rescued the mutant's motility defect back to control levels (Figure 2, C–E). This site-of-action analysis revealed overlapping roles for *frpr-14*-expressing interneurons with AVH exerting more comprehensive control over the behavioral repertoire examined in this study compared with AIB (Figure 2F). An

Downloaded from https://academic.oup.com/genetics/article/220/1/iyab198/6422542 by guest on 18 April 2024

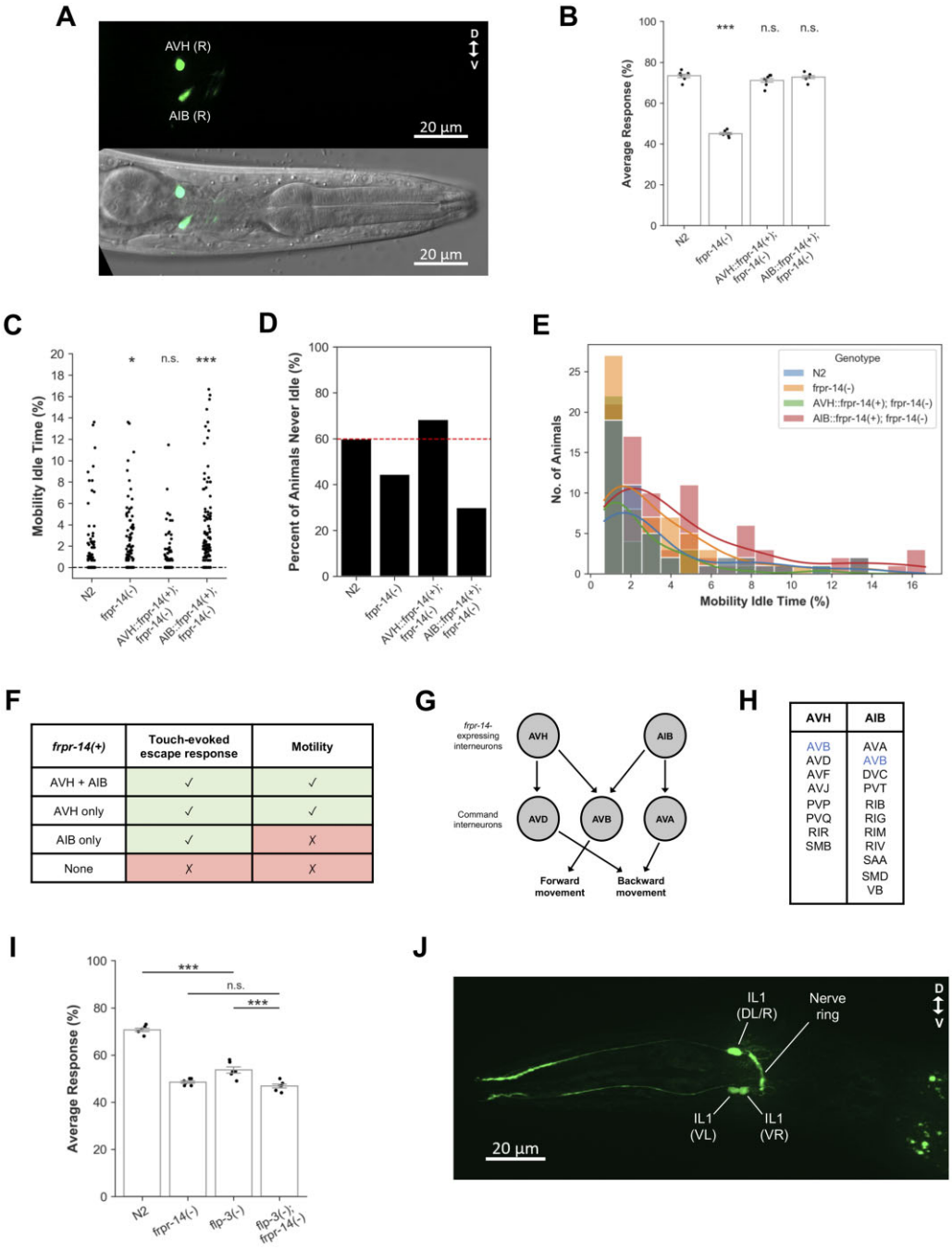

frpr-14(+)	Touch-evoked escape response	Motility
AVH + AIB	✓	✓
AVH only	✓	✓
AIB only	✓	✗
None	✗	✗

AVH	AIB
AVB	AVA
AVD	AVB
AVF	DVC
AVJ	PVT
PVP	RIB
PVQ	RIG
RIR	RIM
SMB	RIV
	SAA
	SMD
	VB

Figure 2 FRPR-14 modulates precommand interneuron function during touch-evoked escape response and motility behaviors. (A) Representative image of *frpr-14* translational GFP reporter expression in L4 stage animal. Top—GFP only. Bottom—DIC and GFP merge. (B) Touch-evoked escape response results for AVH and AIB-specific *frpr-14* cDNA expression in *frpr-14*(−) background. Error bars represent standard error of the mean. $N = 7$ batches. One-way ANOVA followed by Tukey's HSD *post hoc*. Only statistical comparisons to N2 shown. ***$P < 0.001$, n.s., no significance. N2—*frpr-14*(−) ($P = 2.109e{-}14$), N2—AVH::*frpr-14*(+); *frpr-14*(−) ($P = 2.264e{-}01$), N2—AIB::*frpr-14*(+); *frpr-14*(−) ($P = 9.360e{-}01$). (C) Percentage of mobility idle time throughout recording duration. $N = 117$–120 animals. Kruskal–Wallis test followed by Dunn's *post hoc* (Holm–Bonferroni correction). Only statistical comparisons to N2 shown. *$P < 0.05$; ***$P < 0.001$; n.s., no significance. N2—*frpr-14*(−) ($P = 3.924e{-}02$), N2—AVH::*frpr-14*(+); *frpr-14*(−) ($P = 1.108e{-}01$), N2—AIB::*frpr-14*(+); *frpr-14*(−) ($P = 1.123e{-}06$). (D) Percent of animals in (C) that were never idle (*i.e.*, Mobility Idle Time = 0). (E) Distribution of nonzero mobility idle times in (C). Colored lines represent kernel density estimation. $N = 38$–84 animals. (F) Summary of *frpr-14* site-of-action analysis. (G) Schematic showing synaptic connections between *frpr-14*-expressing interneurons and command interneurons (White *et al.* 1986). Arrows represent chemical synapses. Connections are unweighted. (H) Interneuron and motorneuron classes postsynaptic to AVH and AIB (White *et al.* 1986). Only connections with more than one chemical and/or electrical synapse included. (I) *flp-3*(−); *frpr-14*(−) genetic epistasis analysis for touch-evoked escape response. Error bars represent standard error of the mean. $N = 6$ batches. One-way ANOVA followed by Tukey's HSD *post hoc*. ***$P < 0.001$; n.s., no significance. N2—*flp-3*(−) ($P = 1.942e{-}10$), *flp-3*(−)—*flp-3*(−); *frpr-14*(−) ($P = 2.279e{-}04$), *frpr-14*(−)—*flp-3*(−); *frpr-14*(−) ($P = 5.904e{-}01$). (J) Representative image of *flp-3* transcriptional GFP reporter expression in L4 stage animal. Expression in IL1(L/R) is highly variable, and when present, very weak.

Downloaded from https://academic.oup.com/genetics/article/220/1/iyab198/6422542 by guest on 18 April 2024

examination of the synaptic connections between *frpr-14*-expressing interneurons and the premotor command interneurons provides some clues as to how this cellular context-dependent phenotypic specificity is achieved. AVH and AIB synaptic inputs converge only on AVB, which drives forward movement together with PVC (Figure 2G) (Chalfie *et al.* 1985; White *et al.* 1986). Other than AVB, both *frpr-14*-expressing interneurons do not share any significant downstream synaptic targets (Figure 2H) (White *et al.* 1986). Furthermore, AVH and AIB do not form any synapses with each other (White *et al.* 1986). In the absence of AVH modulation, FRPR-14-mediated AIB activity can act as an alternate driver of the escape response but not spontaneous motility perhaps due to the lack of necessary connections with an AVH-specific motility circuit module. From an ethological perspective, the functional redundancy of AVH and AIB in the escape response but not spontaneous motility makes sense as successful timely escapes from predators is critical for survival while disrupted locomotion patterns during foraging for resources does not pose any imminent danger. An additional network of neuropeptide-mediated extrasynaptic connections might also exist between the *frpr-14*-expressing interneurons and the command interneurons, potentially modulating the cellular responses of this integrative processing layer.

The *C. elegans frpr* gene family is related to the *Drosophila* FMRFamide receptor *FR*, and members of the *frpr* family are predicted to encode cognate receptors for FMRFamide-like peptides encoded by the *flp* gene family (Meeusen *et al.* 2002; Hobert 2013). To identify potential *frpr-14* interactors, we first screened 26 *flp* mutants by visual inspection for a similar decreased motility phenotype as *frpr-14* mutants (Supplementary Table S1). Three candidates, *flp-3*, *flp-4*, and *flp-6*, were then challenged with the touch-evoked escape response assay and we found that all three are defective relative to control animals. Double mutant epistasis analysis revealed that *flp-4(–); frpr-14(–)* and *flp-6(–); frpr-14(–)* animals had significantly enhanced touch-evoked response defects compared with the single mutants (Supplementary Figure S3, A and B) while *flp-3(–); frpr-14(–)* animals phenocopied the *frpr-14* mutant's phenotype (Figure 2I). This suggests that *flp-3* is in the same genetic pathway as *frpr-14* and likely upstream based on the nature of their gene products. In addition to other neuron classes, *flp-3* is expressed in the IL1 head mechanosensory neurons (Figure 2J) (Kim and Li 2004), which regulate the head-withdrawal reflex in response to gentle touches to the side of the animal's head via the RMD motor neurons (Hart *et al.* 1995). Laser microbeam ablation of IL1 also decreases spontaneous head oscillations during foraging (Hart *et al.* 1995). Interestingly, IL1 does not make any synaptic connections with the *frpr-14*-expressing AVH and AIB interneurons (White *et al.* 1986). Thus, a pathway involving *flp-3* and *frpr-14* might couple anatomically distinct touch-evoked escape and motility circuits to coordinate appropriate whole-animal behavioral responses. Further experiments will need to be performed to determine if FLP-3 and FRPR-14 directly interact at the protein level.

Caenorhabditis briggsae is a closely related free-living species that diverged from *C. elegans* at least 18 million years ago (Stein *et al.* 2003; Cutter 2008). Although comparative developmental studies between both species have described conserved and divergent regulatory mechanisms, much less is known about how their neurobehavioral programs are related (Rudel and Kimble 2001; Haag *et al.* 2002; Wang and Chamberlin 2002; Kirouac and Sternberg 2003; Baird *et al.* 2005; Nayak *et al.* 2005; Inoue *et al.* 2007). We used the *C. briggsae* AF16 tropical strain as our reference strain (Stein *et al.* 2003). We wondered if *C. briggsae*'s receptor ortholog *Cbr-frpr-14* regulates the same behaviors as in *C. elegans* and whether *Cbr-frpr-14* modulates the function of similar neuron types (Supplementary Figure S4). *Cbr-frpr-14* is expressed in a single bilaterally symmetric pair of interneurons with cell bodies located in the same relative anatomical positions as the AVH interneurons in *C. elegans* (Figure 3A) (White *et al.* 1986). The processes of these *C. briggsae* AVH-like interneurons also enter the nerve ring before extending into the ventral nerve cord (Figure 3A) (White *et al.* 1986). To determine the physiological relevance of this receptor in *C. briggsae*, we again applied a CRISPR homology-directed repair strategy to generate *Cbr-frpr-14* putative null mutants (Figure 3B) (Cohen and Sternberg 2019). We then assayed these mutants using the touch-evoked escape response and motility assays under the same experimental conditions as *C. elegans*. Both *Cbr-frpr-14* mutant strains had a significantly decreased touch-evoked escape response compared with the *C. briggsae* AF16 wild-type strain, and this difference was more subtle compared with *C. elegans* (Figure 3C). Although overall *Cbr-frpr-14* mutant mobility idle time was not significantly different from control animals, the percentage of *Cbr-frpr-14* mutants that were never idle was consistently lower than the AF16 wild-type control (Figure 3, D–F). Thus, FRPR-14 receptor orthologs modulate the function of a homologous interneuron class to regulate the same behaviors in two *Caenorhabditis* sibling species to different extents. Assuming that all relevant *Cbr-frpr-14* cis-regulatory elements are present in our translational reporter construct, *Cbr-frpr-14* expression in only an AVH-like pair indicates that there is no alternative CBR-FRPR-14-mediated neural pathway to drive the *C. briggase* touch-evoked escape response in the absence of the AVH-like neurons' receptor-mediated functionality. We speculate that either this circuit degeneracy has been selected against in *C. briggsae*'s natural environment or other receptor–neuron pairing(s) play this role in *C. briggsae*.

Despite the high conservation of the FLP peptide repertoire between *Caenorhabditis* species (Li and Kim 2014), whether orthologous ligand–receptor relationships are also conserved has never been experimentally probed *in vivo*. We found that AVH-specific *Cbr-frpr-14* cDNA expression in the *C. elegans frpr-14* mutant was sufficient to fully rescue both touch-evoked escape and motility defects suggesting full conservation of this ligand–receptor interaction between both *Caenorhabditis* species (Figure 4, B and E–G). Electron microscopy-based reconstruction of the *P. pacificus* sensory nervous system indicates that *P. pacificus* and *C. elegans*, which diverged ∼100 million years ago, share similar overall synaptic connectivity structures (Hong *et al.* 2019). How then might numerically constrained nervous systems reconfigure sensorimotor information flow to generate species-specific behavioral variation during evolutionary adaptation? Changes in neuropeptide ligand/receptor coding sequences that affect their protein interactions and changes in *cis/trans*-regulatory elements that determine ligand/receptor spatial expression patterns represent two alternative circuit "rewiring" strategies impinging upon extrasynaptic neuropeptide signaling networks. Our results suggest that, in the context of the touch-evoked escape circuit, the latter strategy is employed. *Cis/trans*-regulatory evolution has also been previously reported to underlie phenotypic divergence between sibling species of both *Caenorhabditis* and *Drosophila* (Sucena and Stern 2000; Wang and Chamberlin 2002; Ortiz *et al.* 2006; Nagy *et al.* 2018; Prabh *et al.* 2018).

As a subset of *C. elegans flp* genes, including *flp-3*, have sequelogs in parasitic species (McCoy *et al.* 2014), we further extended our cross-species receptor expression analysis to *frpr-14* orthologs of the filarial parasites *Brugia malayi* and *Onchocerca volvulus*

Downloaded from https://academic.oup.com/genetics/article/220/1/iyab198/6422542 by guest on 18 April 2024

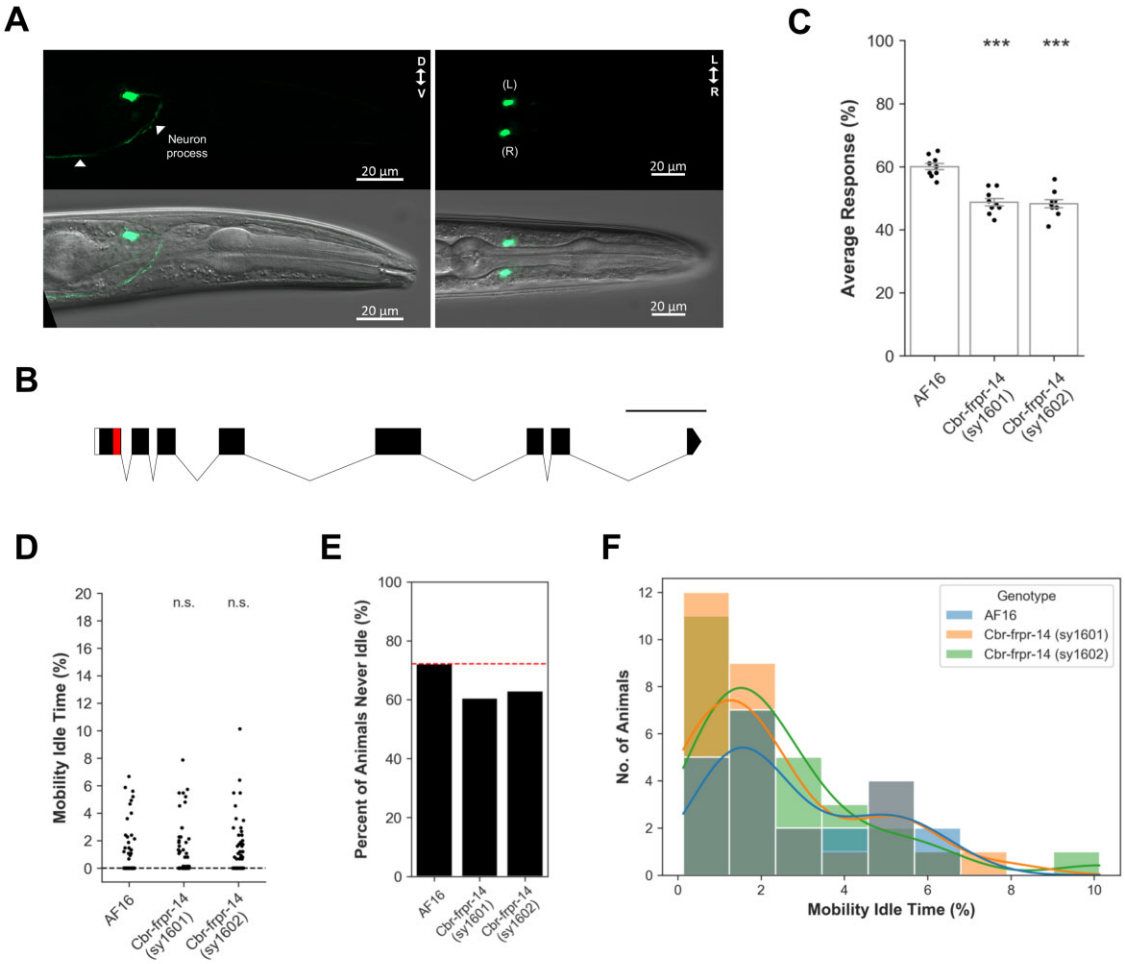

Figure 3 *Cbr-frpr-14* regulates the same behaviors in *C. briggsae* via modulation of an AVH-like interneuron pair. (A) Representative image of *Cbr-frpr-14* translational GFP reporter expression in young adult stage animal. Top—GFP only. Bottom—DIC and GFP merge. (B) Schematic depicting stop cassette insertion site (red) near the end of *Cbr-frpr-14*'s first exon. Scale bar represents 500 bp. (C) Touch-evoked escape response assay for *Cbr-frpr-14* null mutants. Error bars represent standard error of the mean. $N = 9$ batches. One-way ANOVA followed by Dunnett's *post hoc* compared with AF16. ***$P < 0.001$. *Cbr-frpr-14* (*sy1601*) ($P = 2.8e{-}06$), *Cbr-frpr-14* (*sy1602*) ($P = 1.6e{-}06$). (D) Percentage of mobility idle time throughout recording duration. $N = 76$–81 animals. Kruskal–Wallis test followed by Dunn's *post hoc* (Holm–Bonferroni correction). Only statistical comparisons to N2 shown. n.s., no significance. AF16—*Cbr-frpr-14* (*sy1601*) ($P = 7.273e{-}01$), AF16—*Cbr-frpr-14* (*sy1602*) ($P = 6.402e{-}01$). (E) Percent of animals in (D) that were never idle (*i.e.*, Mobility Idle Time = 0). (F) Distribution of nonzero mobility idle times in (E). Colored lines represent kernel density estimation. $N = 22$–30 animals.

(Figure 4A). Surprisingly, we observed almost full (~77%) rescue of the mutant's touch-evoked escape response defect by AVH-specific *Bma-frpr-14* expression but a complete absence of a motility defect rescue (Figure 4, C and E–G). The simplest explanation for this result is that differences between *C. elegans* and *B. malayi* orthologous receptor binding site residues lead to decreased *C. elegans* endogenous neuropeptide ligand efficacy (partial agonism) and weaker activation of BMA-FRPR-14 (Weis and Kobilka 2018). This difference could have shifted AVH neural activity in excess of some threshold to partially trigger the escape response but was insufficient to affect the mutant's motility defect. AVH-specific expression of the most distantly related *Ovo-frpr-14* cDNA did not rescue the *C. elegans frpr-14* mutant's touch-evoked response defect (Figure 4D). Although this study does not further pursue the mechanisms underlying the functional differences between these receptor orthologs (Figure 4H), we propose this experimental paradigm as a tractable *in vivo* system for future studies on how related receptor sequences expressed in the same cellular context can produce specific behavioral outputs.

Through systematic behavioral screening of neuropeptide receptor mutants followed by expression pattern analysis of candidate receptors, we have implicated new neuron classes in the circuitry controlling the *C. elegans* body touch-evoked escape response. Our approach and findings underscore the value of functional genetic screens in the discovery of novel circuit elements. We further show that the receptor mutant with the most severe phenotype, *frpr-14*, also has a spontaneous motility defect and that FRPR-14 signaling via different interneuron classes can drive distinct behavioral subsets. Future studies will elucidate whether and how this cellular context-dependent phenotypic specificity arises from the interplay between receptor site of action and the animal's hardwired neural architecture.

By applying precision genome editing to perturb *Cbr-frpr-14* function in *C. briggsae*, we directly show that orthologous interneuron neuropeptide receptors regulate the same behaviors in two closely related *Caenorhabditis* species but to different extents. Our results also suggest that changes in neuropeptide receptor

Downloaded from https://academic.oup.com/genetics/article/220/1/iyab198/6422542 by guest on 18 April 2024

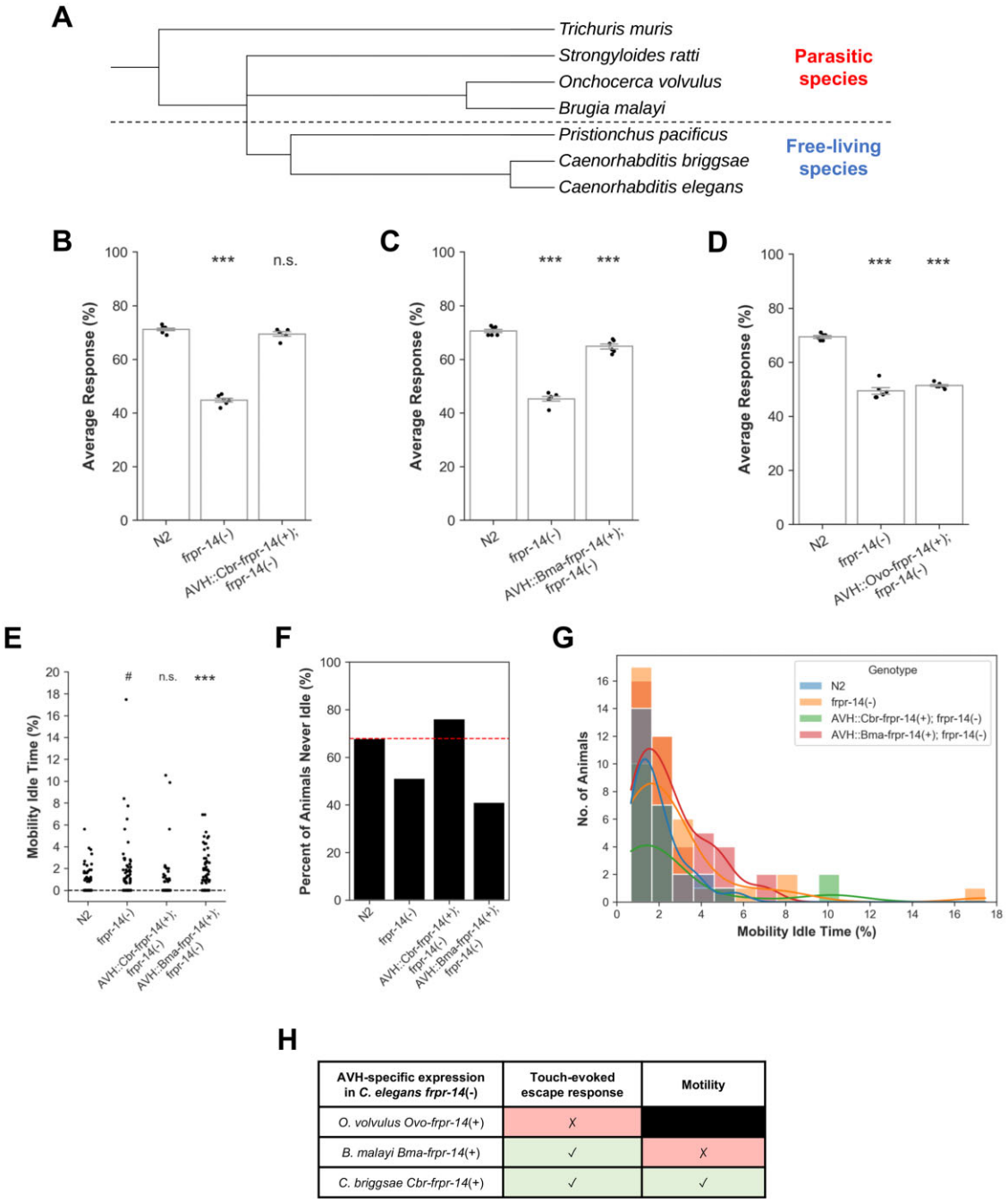

AVH-specific expression in *C. elegans frpr-14(-)*	Touch-evoked escape response	Motility
O. volvulus Ovo-frpr-14(+)	✗	
B. malayi Bma-frpr-14(+)	✓	✗
C. briggsae Cbr-frpr-14(+)	✓	✓

Figure 4 FRPR-14 ortholog-mediated *C. elegans* AVH behavioral output range decreases with evolutionary distance. (A) Phylogenetic tree showing selected free-living and parasitic species of the nematode phylum. Touch-evoked escape response assay for cross-species AVH-specific *Cbr-* or *Bma-* or *Ovo-frpr-14* cDNA expression in *C. elegans frpr-14(−)* background. Error bars represent standard error of the mean. $N = 5$–6 batches. One-way ANOVA followed by Tukey's HSD *post hoc*. Only statistical comparisons to N2 shown. ***$P < 0.001$; n.s., no significance. (B) *Caenorhabditis briggsae Cbr-frpr-14* cDNA. N2—*frpr-14(−)* ($P = 9.155e-13$), N2—AVH::*Cbr-frpr-14(+)*; *frpr-14(−)* ($P = 2.813e-01$). (C) Brugia *malayi Bma-frpr-14* cDNA. N2—*frpr-14(−)* ($P = 5.531e-12$), N2—AVH::*Bma-frpr-14(+)*; *frpr-14(−)* ($P = 7.808e-04$). (D) Onchocerca *volvulus Ovo-frpr-14* cDNA. N2—*frpr-14(−)* ($P = 5.445e-11$), N2—AVH::*Ovo-frpr-14(+)*; *frpr-14(−)* ($P = 2.458e-10$). (E) Percentage of mobility idle time throughout recording duration. $N = 73$–84 animals. Kruskal–Wallis test followed by Dunn's *post hoc* (Holm–Bonferroni correction). Only statistical comparisons to N2 shown. #$P < 0.1$; **$P < 0.01$; n.s., no significance. N2—*frpr-14(−)* ($P = 7.256e-02$), N2—AVH::*Cbr-frpr-14(+)*; *frpr-14(−)* ($P = 3.186e-01$), N2—AVH::*Bma-frpr-14(+)*; *frpr-14(−)* ($P = 1.1556e-03$). (F) Percent of animals in (E) that were never idle (*i.e.*, Mobility Idle Time = 0). (G) Distribution of nonzero mobility idle times (F). Colored lines represent kernel density estimation. $N = 20$–43 animals. (H) Summary of *C. elegans frpr-14(−)* AVH-specific *frpr-14* ortholog cDNA expression analysis.

expression, but not ligand–receptor interactions, underlie species-specific differences in touch-evoked escape circuit architecture. Synapse formation, maintenance, and information transmission are metabolically costly (Laughlin 2001; Laughlin and Sejnowski 2003). Extrasynaptic neuropeptide signaling helps to minimize this metabolic load by "wirelessly" expanding short and long-range neural connectivity and by increasing the modularity of the hard-wired connectome. By examining the function and site of action of an interneuron neuropeptide receptor along two dimensions, behavior and species, we have shed light on the principles used by a compact brain to generate intraspecific behavioral complexity and interspecific variation.

Downloaded from https://academic.oup.com/genetics/article/220/1/iyab198/6422542 by guest on 18 April 2024

Data availability

Strains and plasmids are available upon request. The authors affirm that all data necessary for confirming the conclusions of the article are present within the article, figures, and tables.

Supplementary material is available at *GENETICS* online.

Acknowledgments

Some strains were provided by the CGC, which is funded by NIH Office of Research Infrastructure Programs (P40 OD010440). WormBase provided key molecular and genetic information. Some strains were provided by the lab of Dr Shohei Mitani as part of the National Bioresource Project. We thank Shu Fay Ung for generating the schematic in Figure 1A.

Conceptualization—C.M.C. and P.W.S. Experimental design and data analysis—C.M.C., W.C., W.W., and X.W. Molecular cloning and transgenesis—C.M.C. *Caenorhabditis elegans* CRISPR mutagenesis—H.P. *Caenorhabditis briggsae* CRISPR mutagenesis—S.M.C. Touch-evoked escape response assays—W.C. Motility assays—W.W. Male mating assays—X.W. Microscopy and neuron identification—C.M.C. C.M.C. wrote the paper with input from all coauthors. Funding acquisition—P.W.S.

Funding

This work was funded by NIH grants R240D023041 and R01NS113119 to P.W.S.

Conflicts of interest

The authors declare that there is no conflict of interest.

Literature cited

Baird SE, Davidson CR, Bohrer JC. 2005. The genetics of ray pattern variation in *Caenorhabditis briggsae*. BMC Evol Biol. 5:3.

Barr MM, Sternberg PW. 1999. A polycystic kidney-disease gene homologue required for male mating behaviour in *C. elegans*. Nature. 401:386–389.

Bendena WG, Boudreau JR, Papanicolaou T, Maltby M, Tobe SS, *et al.* 2008. A *Caenorhabditis elegans* allatostatin/galanin-like receptor NPR-9 inhibits local search behavior in response to feeding cues. Proc Natl Acad Sci USA. 105:1339–1342.

Bento G, Ogawa A, Sommer RJ. 2010. Co-option of the hormone-signalling module dafachronic acid-DAF-12 in nematode evolution. Nature. 466:494–497.

Card GM. 2012. Escape behaviors in insects. Curr Opin Neurobiol. 22: 180–186.

Chalfie M, Sulston J. 1981. Developmental genetics of the mechanosensory neurons of *Caenorhabditis elegans*. Dev Biol. 82:358–370.

Chalfie M, Sulston JE, White JG, Southgate E, Thomson JN, *et al.* 1985. The neural circuit for touch sensitivity in *Caenorhabditis elegans*. J Neurosci. 5:956–964.

Chao MY, Komatsu H, Fukuto HS, Dionne HM, Hart AC. 2004. Feeding status and serotonin rapidly and reversibly modulate a *Caenorhabditis elegans* chemosensory circuit. Proc Natl Acad Sci USA. 101:15512–15517.

Chatzigeorgiou M, Grundy L, Kindt KS, Lee WH, Driscoll M, *et al.* 2010. Spatial asymmetry in the mechanosensory phenotypes of the *C. elegans* DEG/ENaC gene mec-10. J Neurophysiol. 104:3334–3344.

Chen X, Chalfie M. 2014. Modulation of *C. elegans* touch sensitivity is integrated at multiple levels. J Neurosci. 34:6522–6536.

Cho JY, Sternberg PW. 2014. Multilevel modulation of a sensory motor circuit during *C. elegans* sleep and arousal. Cell. 156:249–260.

Choi S, Chatzigeorgiou M, Taylor KP, Schafer WR, Kaplan JM. 2013. Analysis of NPR-1 reveals a circuit mechanism for behavioral quiescence in *C. elegans*. Neuron. 78:869–880.

Cohen S, Sternberg P. 2019. Genome editing of *Caenorhabditis briggsae* using CRISPR/Cas9 co-conversion marker dpy-10. MicroPubl Biol. 2019.

Cook SJ, Vidal B, Hobert O. 2021. The bHLH-PAS gene hlh-34 is expressed in the AVH, not AVJ interneurons. MicroPubl Biol. 2021.

Cutter AD. 2008. Divergence times in *Caenorhabditis* and *Drosophila* inferred from direct estimates of the neutral mutation rate. Mol Biol Evol. 25:778–786.

Frooninckx L, Van Rompay L, Temmerman L, Van Sinay E, Beets I, *et al.* 2012. Neuropeptide GPCRs in *C. elegans*. Front Endocrinol (Lausanne). 3:167.

Haag ES, Wang S, Kimble J. 2002. Rapid coevolution of the nematode sex-determining genes fem-3 and tra-2. Curr Biol. 12:2035–2041.

Hart AC, Sims S, Kaplan JM. 1995. Synaptic code for sensory modalities revealed by *C. elegans* GLR-1 glutamate receptor. Nature. 378: 82–85.

Herberholz J, Marquart GD. 2012. Decision making and behavioral choice during predator avoidance. Front Neurosci. 6:125.

Hobert O. 2013. The neuronal genome of *Caenorhabditis elegans*. WormBook. 1–106.

Hong RL, Riebesell M, Bumbarger DJ, Cook SJ, Carstensen HR, *et al.* 2019. Evolution of neuronal anatomy and circuitry in two highly divergent nematode species. Elife. 8.

Inoue T, Ailion M, Poon S, Kim HK, Thomas JH, *et al.* 2007. Genetic analysis of dauer formation in *Caenorhabditis briggsae*. Genetics. 177:809–818.

Kaplan JM, Horvitz HR. 1993. A dual mechanosensory and chemosensory neuron in *Caenorhabditis elegans*. Proc Natl Acad Sci USA. 90:2227–2231.

Karagoz M, Gulcu B, Cakmak I, Kaya HK, Hazir S. 2007. Predation of entomopathogenic nematodes by *Sancassania* sp. (Acari: Acaridae). Exp Appl Acarol. 43:85–95.

Keating CD, Kriek N, Daniels M, Ashcroft NR, Hopper NA, *et al.* 2003. Whole-genome analysis of 60 G protein-coupled receptors in *Caenorhabditis elegans* by gene knockout with RNAi. Curr Biol. 13: 1715–1720.

Kim K, Li C. 2004. Expression and regulation of an FMRFamide-related neuropeptide gene family in *Caenorhabditis elegans*. J Comp Neurol. 475:540–550.

Kirouac M, Sternberg PW. 2003. cis-Regulatory control of three cell fate-specific genes in vulval organogenesis of *Caenorhabditis elegans* and *C. briggsae*. Dev Biol. 257:85–103.

Laughlin SB. 2001. Energy as a constraint on the coding and processing of sensory information. Curr Opin Neurobiol. 11:475–480.

Laughlin SB, Sejnowski TJ. 2003. Communication in neuronal networks. Science. 301:1870–1874.

Li C, Kim K. 2014. Family of FLP peptides in *Caenorhabditis elegans* and related nematodes. Front Endocrinol (Lausanne). 5:150.

Liu KS, Sternberg PW. 1995. Sensory regulation of male mating behavior in *Caenorhabditis elegans*. Neuron. 14:79–89.

Maguire SM, Clark CM, Nunnari J, Pirri JK, Alkema MJ. 2011. The *C. elegans* touch response facilitates escape from predacious fungi. Curr Biol. 21:1326–1330.

McCoy CJ, Atkinson LE, Zamanian M, McVeigh P, Day TA, *et al.* 2014. New insights into the FLPergic complements of parasitic nematodes: informing deorphanisation approaches. EuPA Open Proteom. 3:262–272.

Downloaded from https://academic.oup.com/genetics/article/220/1/iyab198/6422542 by guest on 18 April 2024

Meeusen T, Mertens I, Clynen E, Baggerman G, Nichols R, *et al.* 2002. Identification in *Drosophila melanogaster* of the invertebrate G protein-coupled FMRFamide receptor. Proc Natl Acad Sci USA. 99:15363–15368.

Nagy O, Nuez I, Savisaar R, Peluffo AE, Yassin A, *et al.* 2018. Correlated evolution of two copulatory organs via a single *cis*-regulatory nucleotide change. Curr Biol. 28:3450–3457.e13.

Nath RD, Chow ES, Wang H, Schwarz EM, Sternberg PW. 2016. *C. elegans* stress-induced sleep emerges from the collective action of multiple neuropeptides. Curr Biol. 26:2446–2455.

Nayak S, Goree J, Schedl T. 2005. fog-2 and the evolution of self-fertile hermaphroditism in *Caenorhabditis*. PLoS Biol. 3:e6.

Ortiz CO, Etchberger JF, Posy SL, Frøkjaer-Jensen C, Lockery S, *et al.* 2006. Searching for neuronal left/right asymmetry: genomewide analysis of nematode receptor-type guanylyl cyclases. Genetics. 173:131–149.

Piggott BJ, Liu J, Feng Z, Wescott SA, Xu XZ. 2011. The neural circuits and synaptic mechanisms underlying motor initiation in *C. elegans*. Cell. 147:922–933.

Pirri JK, Alkema MJ. 2012. The neuroethology of *C. elegans* escape. Curr Opin Neurobiol. 22:187–193.

Prabh N, Roeseler W, Witte H, Eberhardt G, Sommer RJ, *et al.* 2018. Deep taxon sampling reveals the evolutionary dynamics of novel gene families in Pristionchus nematodes. Genome Res. 28: 1664–1674.

Rudel D, Kimble J. 2001. Conservation of glp-1 regulation and function in nematodes. Genetics. 157:639–654.

Schwarz J, Lewandrowski I, Bringmann H. 2011. Reduced activity of a sensory neuron during a sleep-like state in *Caenorhabditis elegans*. Curr Biol. 21:R983–R984.

Stein LD, Bao Z, Blasiar D, Blumenthal T, Brent MR, *et al.* 2003. The genome sequence of *Caenorhabditis briggsae*: a platform for comparative genomics. PLoS Biol. 1:E45.

Sucena E, Stern DL. 2000. Divergence of larval morphology between *Drosophila sechellia* and its sibling species caused by cis-regulatory evolution of ovo/shaven-baby. Proc Natl Acad Sci USA. 97: 4530–4534.

Wang H, Park H, Liu J, Sternberg PW. 2018. An efficient genome editing strategy to generate putative null mutants in *Caenorhabditis elegans* using CRISPR/Cas9. G3 (Bethesda). 8:3607–3616.

Wang X, Chamberlin HM. 2002. Multiple regulatory changes contribute to the evolution of the *Caenorhabditis* lin-48 ovo gene. Genes Dev. 16:2345–2349.

Weis WI, Kobilka BK. 2018. The molecular basis of G protein-coupled receptor activation. Annu Rev Biochem. 87:897–919.

White JG, Southgate E, Thomson JN, Brenner S. 1986. The structure of the nervous system of the nematode *Caenorhabditis elegans*. Philos Trans R Soc Lond B Biol Sci. 314:1–340.

Wilecki M, Lightfoot JW, Susoy V, Sommer RJ. 2015. Predatory feeding behaviour in Pristionchus nematodes is dependent on phenotypic plasticity and induced by serotonin. J Exp Biol. 218: 1306–1313.

Xie H, Aminuzzaman FM, Xu L, Lai Y, Li F, *et al.* 2010. Trap induction and trapping in eight nematode-trapping fungi (Orbiliaceae) as affected by juvenile stage of *Caenorhabditis elegans*. Mycopathologia. 169:467–473.

Yang CT, Vidal-Diez de Ulzurrun G, Gonçalves AP, Lin HC, Chang CW, *et al.* 2020. Natural diversity in the predatory behavior facilitates the establishment of a robust model strain for nematode-trapping fungi. Proc Natl Acad Sci USA. 117: 6762–6770.

Zheng Y, Brockie PJ, Mellem JE, Madsen DM, Maricq AV. 1999. Neuronal control of locomotion in *C. elegans* is modified by a dominant mutation in the GLR-1 ionotropic glutamate receptor. Neuron. 24:347–361.

Communicating editor: A. Barrios

Downloaded from https://academic.oup.com/genetics/article/220/1/iyab198/6422542 by guest on 18 April 2024